PHYSICAL REVIEW C **95**, 061304(R) (2017)

Jacobi-type transitions in the interacting boson model

Y. Zhang[1,2,*] and F. Iachello[2,†]

[1]*Department of Physics, Liaoning Normal University, Dalian 116029, People's Republic of China*

[2]*Center for Theoretical Physics, Sloane Physics Laboratory, Yale University, New Haven, Connecticut 06520-8120, USA*

(Received 24 February 2017; published 7 June 2017)

We examine, within the framework of the interacting boson model, the structural evolution along the excitation energy across the saddle points of potential wells in a finite nuclear system, and its connection with excited-state quantum phase transitions (ESQPTs). We find that transitions between γ-rigid and γ-soft shapes occur as a function of angular momentum, L, analogous to the Jacobi transitions occurring in rotating stars. Empirical evidence of these transitions is found in the rotational spectra of $^{156-162}$Gd.

DOI: 10.1103/PhysRevC.95.061304

In recent years, quantum phase transitions (QPTs) have become an important subject of investigation in many fields of physics. QPTs describe changes in the ground-state properties of systems at zero temperature, hence the name ground-state, or zero-temperature, quantum phase transitions (GSQPTs) given to them. Although a definition of phase transition in terms of singularities implies infinite systems, nonetheless the main features of GSQPTs have been found to persist even for mesoscopic systems with $N \sim 10$ [1]. Sudden changes in the effective order parameters (observables sensitive to QPT) as a function of the control parameters are identified as precursors of GSQPTs defined in the large-N limit. Nuclei provide rich examples of such GSQPTs, and the related topics have been widely discussed in the past two decades [2–4].

Considerable attention has very recently been given to the so-called excited-state QPT (ESQPT) [5–13]. Unlike GSQPT, an ESQPT can occur not only with variation of the control parameters of a model Hamiltonian but also with increasing excitation energy. ESQPTs in a given system are deeply rooted in the corresponding GSQPT, and they can be considered as an extension of the GSQPT toward excited states. Algebraic approaches provide convenient ways to investigate both GSQPTs and ESQPTs in mesoscopic systems. The best examples are the interacting boson model (IBM) [14] for nuclear structure and the vibron model (VM) [15] for molecules and atomic clusters. Evidence of the ESQPT associated with the GSQPT in the VM [9,10] has been identified from the bending motions in nonrigid molecules [16,17]. However, there is still no experimental evidence reported for ESQPT in nuclei despite the fact that model calculations within the IBM have shown that more abundant ESQPTs are present in the large-N limit of this model [13].

In this work, we investigate whether ESQPTs in the IBM survive in a realistic situation as the GSQPTs did [1], and we discern possible fingerprints of ESQPT in deformed nuclei. In particular, we study transitions that occur as a function of the angular momentum, L, from γ-stable, $\gamma = 0^\circ$, to γ-unstable, $\langle\gamma\rangle = 30^\circ$, structures. These transitions are analogous to those which occur in gravitating rotating stars, where they are known as Jacobi transitions [18]. Several studies of Jacobi transitions in nuclei have been done [19–24]. In these studies within the framework of the liquid drop model, Jacobi transitions from oblate to triaxial shapes occur in rotating nuclei at typical values of $L \sim 60$. Here we show that similar phenomena occur at lower values of the angular momentum, $L \sim 8$, specifically transitions from axially deformed prolate to γ-unstable shapes, with the framework of the interacting boson model. Since these are similar but not identical to those discussed previously [19–24], we denote them here as Jacobi-type instead of simply Jacobi transitions. We also show that these transitions can be related to precursors of ESQPTs only in a small region of the IBM phase diagram and are otherwise gradual changes in the evolution with angular momentum.

A Hamiltonian in the IBM framework is constructed from two kinds of boson operator, s boson with $J^\pi = 0^+$ and d boson with $J^\pi = 2^+$ [14]. Specifically, we consider the IBM consistent-Q Hamiltonian [25]

$$\hat{H}(\eta,\chi) = \epsilon\left[(1-\eta)\hat{n}_d - \frac{\eta}{4N}\hat{Q}^\chi\cdot\hat{Q}^\chi\right], \tag{1}$$

where $\hat{n}_d$ and $\hat{Q}^\chi = (d^\dagger s + s^\dagger\tilde{d})^{(2)} + \chi(d^\dagger\tilde{d})^{(2)}$ with $\eta \in [0,1]$ and $\chi \in [-\sqrt{7}/2, 0]$. The dynamical structures of this Hamiltonian are controlled by two parameters (apart from a scale factor ϵ), η and χ. It can be proved that the Hamiltonian is in the U(5) dynamical symmetry (DS) when $\eta = 0$, in the SO(6) DS when $\eta = 1$ and $\chi = 0$, and in the SU(3) DS when $\eta = 1$ and $\chi = -\frac{\sqrt{7}}{2}$. Its classical limit (Landau potential) can be obtained by the method of coherent states in terms of two classical coordinates β and γ. The scaled potential energy surface, $E(\beta,\gamma)/\epsilon N$, is given by [1]

$$\begin{aligned} V(\beta,\gamma) = {} & \frac{\beta^2}{1+\beta^2}\left[(1-\eta) - (\chi^2+1)\frac{\eta}{4N}\right] \\ & - \frac{5\eta}{4N(1+\beta^2)} - \frac{\eta(N-1)}{4N(1+\beta^2)^2} \\ & \times\left[4\beta^2 - 4\sqrt{\frac{2}{7}}\chi\beta^3\cos 3\gamma + \frac{2}{7}\chi^2\beta^4\right]. \end{aligned} \tag{2}$$

To determine types and orders of the GSQPTs, one minimizes the potential function in (2) by varying β and γ for given η and χ. The optimal values are denoted as β_e and γ_e, with which one can get the ground-state energy per boson

*dlzhangyu_physics@163.com

†francesco.iachello@yale.edu

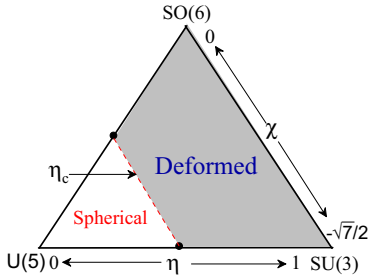

FIG. 1. The phase diagram of the IBM.

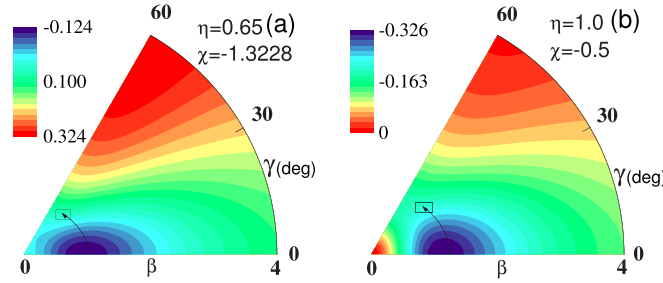

FIG. 2. Potential energy surfaces ($N = 15$), according to Eq. (2), for the selected two cases.

defined as $E_g = V(\eta,\chi,\beta_e,\gamma_e)$. For second-order QPT, E_g and $\frac{\partial E_g}{\partial x}$ are continuous, but $\frac{\partial^2 E_g}{\partial x^2}$ is not, where x represents the corresponding control parameter. For first-order QPT, E_g is continuous, but $\frac{\partial E_g}{\partial x}$ is not. Based on these criteria [14], one can prove that the first-order GSQPTs occur in the large-N limit at the critical point $\eta_c = \frac{14}{28+\chi^2}$ with $\chi \in [-\sqrt{7}/2,0]$, which are collectively called spherical-deformed GSQPTs. The two-dimensional phase diagram of the IBM described by (1) can be mapped onto a triangle [25] as shown in Fig. 1, where the critical line denoted by η_c cuts the triangle into two regions, the spherical and deformed. In this diagram, the line of first-order transitions ends at a point of second-order transition at $\eta_c = 0.5, \chi = 0$ [14], namely U(5)-SO(6) GSQPT. Notably, the phase diagram of Fig. 1 should be doubled, if the range of χ is extended to $\chi \in [-\sqrt{7}/2, \sqrt{7}/2]$ [26]. However, because of the Z_2 symmetry, $\chi \to -\chi$, of the potential energy surface (2), we confine our discussion here to $\chi \leqslant 0$. It has been shown [6,9,13] that ESQPTs are associated with GSQPTs of Fig. 1 in the deformed region of the phase diagram. The critical excitation energy, E_c, varies from zero along the critical value, $\eta = \eta_c$, to the top of the spectrum of $\eta = 1$. While a classification of the GSQPTs is feasible by means of the method of coherent states discussed above, a more complicated semiclassical analysis is needed in order to classify the associated ESQPTs [6,7,11–13,27]. In the following, we will focus on (i) identification of signatures of ESQPTs associated with deformed nuclei rather than classification of ESQPTs in the IBM and (ii) whether ESQPTs or their precursors persist for finite N. We will also discuss whether the transitions are phase transitions or simply crossovers.

In order to study whether finite N precursors of ESQPTs occur in the deformed region of the phase diagram, we select two typical parameter points with $(\eta,\chi) = (0.65,-1.3228 \simeq -\frac{\sqrt{7}}{2})$ and $(\eta,\chi) = (1.0,-0.5)$, and $N = 15$. The potential energy contours obtained from (2) for the selected two cases are shown in Fig. 2. As seen from Fig. 2(a), the constant-energy surfaces develop a clear low-energy well (blue color) around $\beta \simeq \sqrt{2}$ and $\gamma = 0^\circ$, which indicates that the states confined in the well are γ rigid [28,29] and associated with the SU(3) quasidynamical symmetry [28,30,31]. Once they are excited out of the low-energy well (as signified with the arrow in Fig. 2), the states may become γ soft since the γ degree of each constant-energy surface outside of the well ranges from 0° to 60°. The γ-soft picture outside of the well in the present case is very similar to that in the spherical region of the triangle, where the γ degree of each constant-energy surface also ranges from 0° to 60° [14]. Hence, the transition from inside to outside of the well as a function of excitation energy is referred to as a γ-rigid to γ-soft transition. The transitional point is defined by

$$E_c(\eta,\chi) = \epsilon N[V(\eta,\chi,\beta_s,\gamma_s) - V(\eta,\chi,\beta_e,\gamma_e)] \qquad (3)$$

with $\frac{\partial V}{\partial \gamma}|_{\beta_s,\gamma_s} = 0$, $\frac{\partial V}{\partial \beta}|_{\beta_s,\gamma_s} = 0$, $\frac{\partial^2 V}{\partial \beta^2}|_{\beta_s,\gamma_s} > 0$, and $\frac{\partial^2 V}{\partial \gamma^2}|_{\beta_s,\gamma_s} < 0$, where $V(\eta,\chi,\beta_s,\gamma_s)$ is the saddle-point energy. Specifically, one gets $E_c = 1.31\epsilon$ for that shown in Fig. 2(a), where the γ-soft picture appearing outside of the well is due to the U(5) DS involved in the Hamiltonian. This transition from SU(3) to U(5) can be regarded as an extension of the U(5)-SU(3) GSQPT along the excitation energy [13]. As seen in Fig. 2(b), there is still a prolate minimum but the transition out of the well occurs at $E_c = 1.76\epsilon$ and is much smoother, indicating a crossover from γ rigid to γ soft rather than a phase transition in accordance to Fig. 1, when going from SU(3) to SO(6). In general, the γ-rigid to γ-soft transition is present in all the deformed region of the phase diagram but with different properties. The γ-soft characteristics may come either from the U(5) or SO(6) DS or their mixing, while the γ-rigid characteristics originate from the SU(3) DS [28,29].

In studying ESQPTs in the IBM, we note that its excitation spectrum consists of vibrational and rotational states. ESQPTs in vibrational and rotational spectra were studied in Ref. [6] within the framework of the U(3) vibron model [32]. By studying the dependence of the gap on excitation energy for various L ($0 \leqslant L \leqslant 15$), as in Fig. 8(c) of Ref. [6], it was found that there is an ESQPT in the vibrational spectra for $L = 0$, and that the singularity at $E = E_c$ disappears for large angular momentum and the transition becomes a crossover. Examples were later found in several molecules [16,17]. In IBM, the nature of the vibrational excitation is more complex than in the vibron model, consisting of β and γ vibrations. Furthermore, the values of $N \sim 10$–20 are smaller than in the vibron model $N \sim 100$. The IBM is thus well suited to study ESQPTs in complex finite-N systems. To this end, we begin by considering the d-boson occupation probability $\rho \equiv \langle L|\hat{n}_d|L\rangle/N$ as the effective order parameter [6,10,13]. This parameter is shown in Fig. 3 as a function of E/ϵ. The behavior of ρ is similar to that of Fig. 8 of Ref. [6] and confirms the result that precursors of ESQPT persist in finite-N systems. However, a detailed analysis of the results shows that the precursors of ESQPT are very clear in Fig. 3(a) at $E_c/\epsilon \approx 1.3$, but that the signatures of ESQPTs gradually disappear when going to Fig. 3(c). This result is consistent with Fig. 2 where

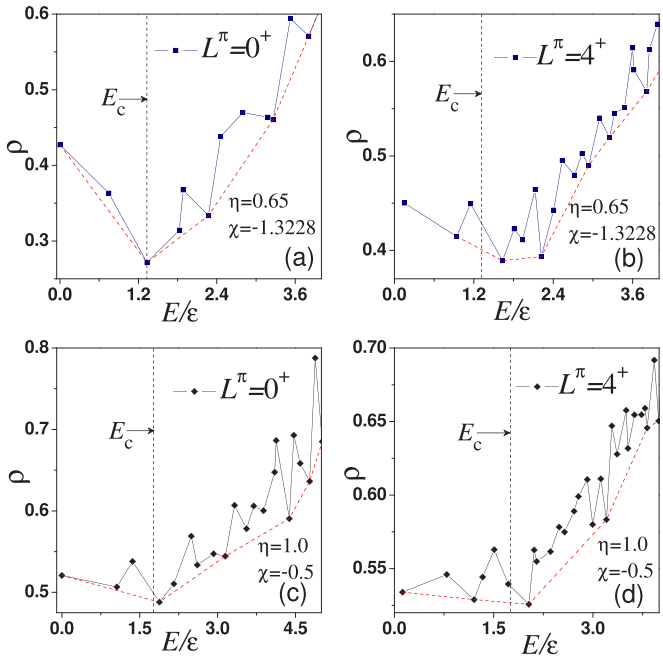

FIG. 3. (a) Behavior of the effective order parameter ρ as a function of the excitation energy for $L^\pi = 0^+$ in the case with $(\eta,\chi) = (0.65,-1.3228)$. (b) The same as in panel (a) but for $L^\pi = 4^+$. (c) Behavior of ρ for $L^\pi = 0^+$ in the case with $(\eta,\chi) = (1.0,-0.5)$. (d) The same as in panel (c) but for $L^\pi = 4^+$. In addition, the dashed red lines are included to guide the eye.

one can see that well is sharper for $\eta = 0.65$, $\chi = -1.3228$ than for $\eta = 1.0$, $\chi = -0.5$, and transitions out of the well are thus sharper in the former case than in the latter case.

We next study the behavior as a function of the angular momentum, L. In order to study this behavior, Regan *et al.* [33] suggested using the quantity $R = \frac{E_\gamma(L\to L-2)}{L}$ [33], where $E_\gamma(L \to L-2)$ represents the γ-ray decay energies, namely the energy difference between the adjacent levels with $\Delta L = 2$ in a given band. One can derive that the quantity R for the ground band is given by $R \propto \frac{1}{L}$ in the U(5) limit, $R \propto (1+\frac{2}{L})$ in the SO(6) limit, and $R \propto (4-\frac{2}{L})$ in the SU(3) limit. It is clear that the values of R in both the U(5) and SO(6) limits monotonically decrease with the increase of the angular momentum L, thus with the rotational excitation energy, but that they always increase monotonically in the SU(3) limit. Although the evolutional behavior of R may change quantitatively away from the symmetry limits, its monotonicity is only determined by the dominant DS. For example, R may keep decreasing as a function of the excitation energy in the whole spherical region as well as the U(5)-SO(6) leg of the triangle, which in turn suggests that the behavior $R \propto (1+\frac{2}{L})$ generated from the $E(L) \propto \tau(\tau+3)$ rule with $\tau = \frac{L}{2}$ in the SO(5) symmetry can be applied to characterize the γ-soft rotational feature caused by either U(5) or SO(6). In short, R increases in the γ-rigid situation [SU(3)-like] but decreases in the γ-soft situation [U(5) or SO(6)-like]. It is thus expected that this qualitative difference can provide a signature for a structural change (γ-rigid to γ-soft) in the rotational excitations of nuclei. To check this point, the evolutionary

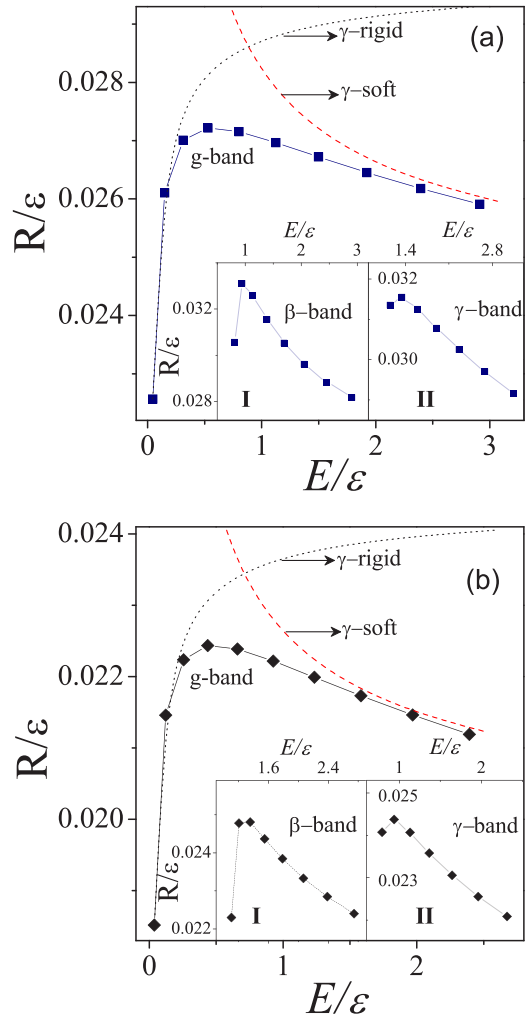

FIG. 4. (a) Behavior of the quantity R/ε as a function of the rotational energy for the ground band (up to $L = 20$) and excited bands (up to $L = 16$) in the case corresponding to $(\eta,\chi) = (0.65,-1.3228)$. The curves denoted by γ rigid and γ soft are those given by $R \propto (4-\frac{2}{L})$ and $R \propto (1+\frac{2}{L})$, respectively. (b) The same as in panel (a) but for $(\eta,\chi) = (1.0,-0.5)$.

behaviors of R as a function of the rotational excitation energy of the ground band and the excited bands in the IBM are shown in Fig. 4, where the behaviors $R \propto (1+\frac{2}{L})$ and $R \propto (4-\frac{2}{L})$ are used to signify the γ-soft and γ-rigid features, respectively. As seen from Fig. 4(a), the values of R in the ground band rapidly grow up in a γ-rigid way with the increase of the excitation energy and then suddenly turn to a monotonic decrease as in the γ-soft way. The changes in monotonicity are also present in the rotational spectra for both the β band and γ band, as shown in the inset. A similar picture could be found from Fig. 4(b), where the sudden change in the evolutional behavior of R indicates the occurrence of the γ-rigid to γ-soft transition in the SU(3)-SO(6) leg. More generally, the sudden changes in the monotonicity of the behavior of R widely appear in the deformed region of the phase diagram. In contrast, the behavior of R as a function of the excitation energy in the spherical region as well as in the three symmetry limits of the IBM is always monotonic.

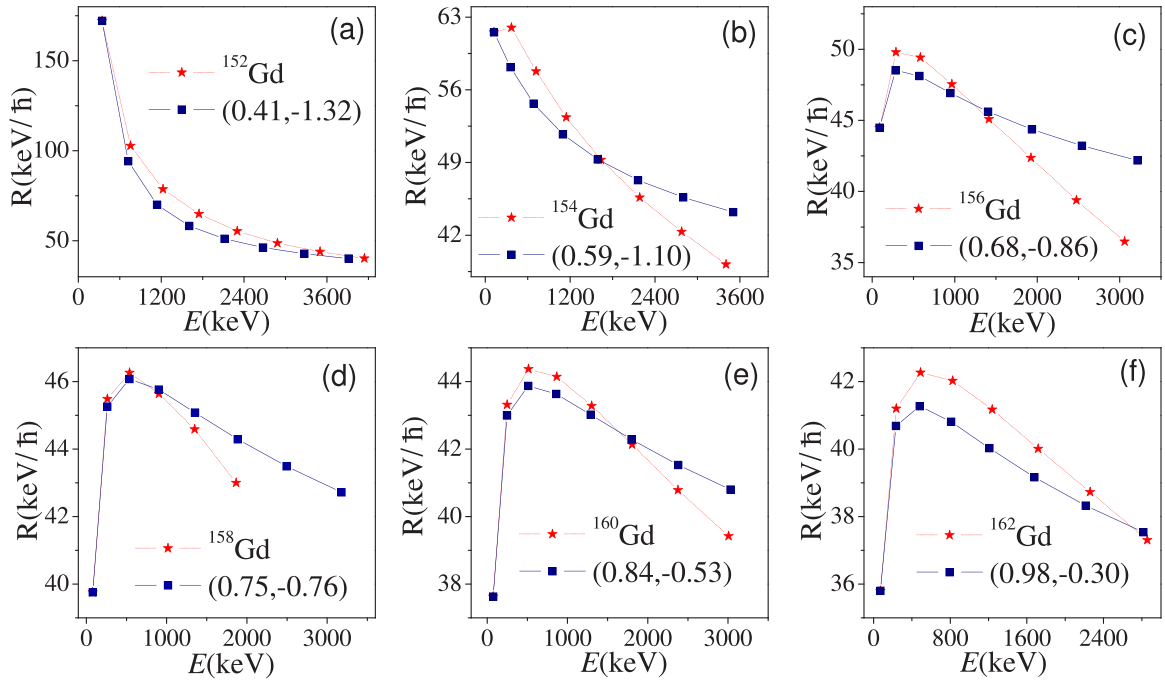

FIG. 5. Comparison between the experimental values of R for the ground bands (up to $L = 16$) in $^{152-162}$Gd [34] and IBM calculations. The scale factor ε is fixed by fitting the experimental values of $E(2_1^+)$ in each case, and values of (η, χ) shown in each panel are taken from Ref. [35] with slightly changes in those for panels (c) and (d).

As discussed above, the γ-rigid to γ-soft transitions in the IBM may persist for a realistic boson number N, so it would be and should be reflected in nuclei. To check this point, we have compared the calculated and experimental [34] R values in $^{152-162}$Gd. The parameters adopted in the calculation are taken from Ref. [35], where the low-lying structures of rare-earth nuclei were well fitted with the IBM Hamiltonian of Eq. (1). As clearly seen from Fig. 5, the experimental data are well described by the IBM calculation. Most importantly, the features of the γ-rigid to γ-soft transitions are clearly seen both in theory and experiment in $^{156-162}$Gd, which lie in the deformed region of the phase diagram [35]. In contrast, as shown in Fig. 5(a) there are not any γ-rigid to γ-soft transitional signals for ^{152}Gd, which lies in the spherical region of the phase diagram, and only incipient signals are seen in ^{154}Gd, which lies on the critical line. A similar conclusion can be drawn from an analysis of nuclei with the neutron number $N_n \geqslant 90$ including $^{152-160}$Sm, $^{158-164}$Dy, $^{160-166}$Er, $^{164-168}$Yb, and ^{168,170}Hf. The γ-rigid to γ-soft transition is instead never found in nuclei with $N_n < 90$ in this mass region. This point fully agrees with the theoretical predictions that the transition from γ rigid to γ soft may occur only to the right of the critical line of the spherically deformed GSQPTs, as nuclei with $N_n = 90$ in the rare-earth region are usually identified as critical point nuclei [2]. It should be also mentioned that the transition occurs much earlier than the back-bending phenomenon due to band crossing. In addition, the back-bending phenomenon along the yrast line often occurs with a transition from vibrational to rotational structures [33], while the γ-rigid to γ-soft transition appears in inverse order, namely from rotational (γ-rigid) to anharmonic vibrational (or γ-soft rotational) patterns. As a result, the transition discussed here is a new phenomenon.

In summary, ESQPT transitional features in IBM have been investigated in realistic situations. It has been found that precursors of ESQPTs persist for finite N with properties analogous to those discussed in Ref. [6]. In addition and most importantly, it has been found that a Jacobi-type transition from axial to triaxial (γ rigid to γ soft) appears at some critical values L_c of the angular momentum in nuclei lying on the deformed side of the phase diagram. Experimental data in the Gd isotopes support this conclusion. The results presented here provide new insight into nuclear structural evolution as a function of angular momentum. When combined with the results of Refs. [19–24], they indicate that this evolution may include several steps, first from the ground-state prolate γ-rigid structure to a γ-unstable structure as discussed here, then from γ-unstable to an oblate structure, and finally to a triaxial structure.

This work was supported in part by US Department of Energy Grant No. DE-FG-02-91ER-40608. One of us (Y.Z.) acknowledges support from the Natural Science Foundation of China (No. 11375005).

[1] F. Iachello and N. V. Zamfir, Phys. Rev. Lett. **92**, 212501 (2004).
[2] P. Cejnar, J. Jolie, and R. F. Casten, Rev. Mod. Phys. **82**, 2155 (2010).
[3] R. F. Casten and E. A. McCutchan, J. Phys. G **34**, R285 (2007).
[4] P. Cejnar and J. Jolie, Prog. Part. Nucl. Phys. **62**, 210 (2009).
[5] P. Cejnar, M. Macek, S. Heinze, J. Jolie, and J. Dobeš, J. Phys. A **39**, L515 (2006).
[6] M. A. Caprio, P. Cejnar, and F. Iachello, Ann. Phys. **323**, 1106 (2008).
[7] P. Cejnar and P. Stránský, Phys. Rev. E **78**, 031130 (2008).
[8] P. Pérez-Fernández, A. Relaño, J. M. Arias, P. Cejnar, J. Dukelsky, and J. E. García-Ramos, Phys. Rev. E **83**, 046208 (2011).
[9] F. Pérez-Bernal and F. Iachello, Phys. Rev. A **77**, 032115 (2008).
[10] F. Pérez-Bernal and O. Álvarez-Bajo, Phys. Rev. A **81**, 050101(R) (2010).
[11] P. Stránský, M. Macek, and P. Cejnar, Ann. Phys. **345**, 73 (2014).
[12] P. Stránský, M. Macek, A. Leviatan, and P. Cejnar, Ann. Phys. **356**, 57 (2015).
[13] Y. Zhang, Y. Zuo, F. Pan, and J. P. Draayer, Phys. Rev. C **93**, 044302 (2016).
[14] F. Iachello and A. Arima, *The Interacting Boson Model* (Cambridge University, Cambridge, UK, 1987).
[15] F. Iachello and R. D. Levine, *Algebraic Theory of Molecules* (Oxford University, Oxford, UK, 1995).
[16] D. Larese and F. Iachello, J. Mol. Struct. **1006**, 611 (2011).
[17] D. Larese, F. Pérez-Bernal, and F. Iachello, J. Mol. Struct. **1051**, 310 (2013).
[18] S. Chandrasekar, *Ellipsoidal Figures of Equilibrium* (Yale University Press, New Haven, CT, 1969).
[19] Y. Alhassid, S. Levit, and J. Zingman, Phys. Rev. Lett. **57**, 539 (1986).
[20] Y. Alhassid and N. Whelan, Nucl. Phys. A **565**, 427 (1993).
[21] D. Ward *et al.*, Phys. Rev. C **66**, 024317 (2002).
[22] K. Mazurek, J. Dudek, A. Maj, and D. Rouvel, Phys. Rev. C **91**, 034301 (2015).
[23] G. Shanmugam, K. Sankar, and K. Ramamurthi, Phys. Rev. C **52**, 1443 (1995).
[24] G. Shanmugam and V. Selvam, Phys. Rev. C **62**, 014302 (2000).
[25] D. D. Warner and R. F. Casten, Phys. Rev. C **28**, 1798 (1983).
[26] J. Jolie, R. F. Casten, P. von Brentano, and V. Werner, Phys. Rev. Lett. **87**, 162501 (2001).
[27] P. Stránský and P. Cejnar, Phys. Lett. A **380**, 2637 (2016).
[28] M. Macek, J. Dobeš, and P. Cejnar, Phys. Rev. C **80**, 014319 (2009).
[29] M. Macek, J. Dobeš, and P. Cejnar, Phys. Rev. C **82**, 014308 (2010).
[30] G. Rosensteel and D. J. Rowe, Nucl. Phys. A **759**, 92 (2005).
[31] D. Bonatsos, E. A. McCutchan, and R. F. Casten, Phys. Rev. Lett. **104**, 022502 (2010).
[32] F. Iachello and S. Oss, J. Chem. Phys. **104**, 6956 (1996).
[33] P. H. Regan *et al.*, Phys. Rev. Lett. **90**, 152502 (2003).
[34] M. J. Martin, Nucl. Data Sheets **114**, 1497 (2013); C. W. Reich, *ibid.* **110**, 2257 (2009); **113**, 2537 (2012); R. G. Helmer, *ibid.* **101**, 325 (2004); C. W. Reich, *ibid.* **105**, 557 (2005); **108**, 1807 (2007).
[35] E. A. McCutchan, N. V. Zamfir, and R. F. Casten, Phys. Rev. C **69**, 064306 (2004).